

Experimental Analysis and Modelling of Solar Panel of Two-Diode Model (TDM) Parameters dependence on various Environmental Temperature and Solar irradiance Changes in Naya Raipur Chhattisgarh

Praveen Kumar Yadaw,
Associate Professor,
Department of Electrical Engineering,
Kalinga University, C.G, India, 492101
werpraveen@gmail.com

Mohammad Arsh Khan, Assistant
Professor, Department of Electrical
Engineering, Kalinga University, C.G,
India, 492101
arsh.khan@kalingauniversity.ac.in

Manoj Kumar Nigam
Professor & Head, Department of
Electrical Engineering, Kalinga
University, Chhattisgarh, India, 492101
manoj.nigam@kalingauniversity.ac.in

Abstract – The growing use of renewable energy sources emphasizes how crucial it is to precisely simulate photovoltaic (PV) systems in order to maximize their efficiency in a variety of environmental settings. Although the two-diode model (TDM) is well known for accurately capturing the behavior of PV modules, environmental unpredictability makes it difficult to extract its parameters. Current approaches frequently aren't flexible enough to handle real-world circumstances like changing temperatures and solar radiation. By creating a hybrid methodology that extracts TDM parameters using both analytical equations and numerical optimization techniques, this study fills this gap. The study was carried out in summertime in Naya Raipur, Chhattisgarh, and found that temperatures fluctuated between 20°C and 31°C and that irradiance levels ranged from 25 W/m² to 245 W/m². The ideality factors (n_1, n_2) were found to range from 2.001 to 2.022 and 0.980 to 1.002, respectively, while important parameters such series resistance (R_s) were fine-tuned to values between 0.333 and 0.368 Ω .

At peak irradiance, the experimental findings showed a maximum power output of 59.77 W, which was in close agreement with MATLAB/Simulink models that had root mean square error (RMSE) values less than 1%. Furthermore, the hybrid methodology outperformed conventional techniques in capturing current-voltage (I-V) characteristics under a variety of environmental circumstances. By bridging the gap between theoretical modeling and real-world

application, the study's results confirm the hybrid methodology as a reliable tool for accurate PV module parameter extraction. This study offers a scalable methodology for enhancing the design of PV systems, facilitating more accurate performance forecasting in practical settings.

Keywords: Photo voltaic (PV), Two- diode model, five-parameter model, Parameter extraction, Analytical modeling, Numerical (NA) techniques, MATLAB/Simulink.

1. Introduction

The effects of global -warming are becoming more and more phenomena obvious today. They have reached every continent and are having a wide range of effects on almost every kind of life on Earth. On the other hand, the growing usage of renewable energy provides a means of substituting clean energy for dirty fossil fuels and safeguarding the environment. Solar photovoltaic (PV) and solar thermal energy are two of these renewable energy sources that have developed significantly in recent decades, with solar PV being especially well-liked and reasonably priced.

The International Renewable Energy Agency reports that as of the end of 2019, 586 GW of grid-connected solar capacity [1] and an additional 3.4 GW of off-grid PV were installed worldwide. One of the least expensive renewable energy (RES) sources is solar photovoltaic technology, and the overall cost of installing solar Project prices are anticipated to drop further, from 340 to 834 USD/KW by 2030 and from 165 to 481USD/KW BY 2050[2].

Researchers have created several algorithms to better understand how photovoltaic systems behave under various operating settings in response to the increased demand for renewable energy sources. Accurate modeling of photovoltaic modules is essential since it allows the industry to maximize solar energy profitability and optimize solar module performance. As a result, numerous techniques for extracting parameters have been created, all to raise the precision and effectiveness of modeling PV systems. [9-14].

By making sure that the simulated I- V curve goes through the open-circuit voltage, short-circuit current, and maximum power on the manufacturer's I- V curve, the analytical method is frequently used for parameter extraction in photovoltaic (PV) modeling. Researchers frequently use approximations to lower the number of unknown factors in order to simplify the equations.

According to some studies, diode one's ideality factor is 1, whereas diode two's ideality factor is greater than 1.2 [16] some people believe that both diodes have the same ideality factor. These presumptions aren't always true. A diode's ideality factor, which quantifies how much its characteristics mirror those of an ideal diode, typically ranges from 1 to 2. No recombination is indicated by a factor of 1, whereas Recombination dominance is indicated by a factor of 2. Mistakes regarding these parameters can have a big impact on how accurate the model is.

Furthermore, some scholars believe that the series (R_s) resistance is 0 while the parallel (R_{sh}) resistance is infinite. This might be the case for a perfect solar cell, but in practice, the series (R_s) resistance relates to the resistance of the several semiconductor layers inside the solar -cell, and the parallel resistance shows leakage across the PN junction. Inaccurate resistance values can affect the precision of the model by decreasing the fill -factor and shifting the maximum Power-Point.

Table 1 The description of various symbols and constants in PV Module

S/N	SYMBOL	DESCRIPTION
1	I	Current of PV module in ampere(A)
2	V	Voltage of PV module in volt(V)
3	P_{mc}	Computed maximum power
4	P_{me}	Experimental maximum power
5	V_m	Maximum voltage
6	I_m	Maximum current
7	V_{oc}	Open circuit voltage
8	I_{sc}	Short circuit current
9	K_v	Temperature coefficient of V_{oc}
10	K_i	Temperature coefficient of I_{sc}
11	STC	Standard test condition
12	N_s	Number of PV cells connected in series
13	R_{sh}	Shunt resistance of PV module
14	R_s	Series resistance of PV module
15	I_{ph}	Light generated current of PV module (photo current)
16	n_1	Diode ideality of diode 1
17	n_2	Diode ideality of diode 2
18	I_{01}	Reverse saturation current if diode 1
19	I_{02}	Reverse saturation current of diode 2
20	T	PV module temperature in kelvin(k)
21	K	Boltzmann constant (1.38×10^{-23} Nm/K)
22	Q	Electron charge (1.6×10^{-19})

Other research makes the assumption that both diodes' saturation currents are equivalent. Nevertheless, there is no physical basis for this assumption. The junction temperature determines the reverse (I_{sh}) saturation current, or leakage current (I_{co}), while the recombination -current, which results in indicating a loss of charge carriers from electron-hole recombination. This approach can have a negative impact on model accuracy because the recombination current is usually significantly higher than their reverse diffusion -currents.

To extract photovoltaic parameters, this work presents a hybrid method that combines analytical and numerical (NA) approaches. It doesn't rely on presumptions or oversimplifications that might lower the accuracy of the results, unlike earlier techniques. By solving a non-linear equation with the “Brent technique”, which combines bi-section, inverse-quadratic interpolation and root bracketing, the analytical method can independently extract parameters. The series resistance value can be attained by solving these equations, and the remaining parameters can then be determined. Using a quick iterative approach to match computed and

experimental powers, seven parameters are recovered using the hybrid method, which yields more accurate findings. The ideal values of the ideality factor and series (R_s) resistance factors are found through an iterative method. Using analytical formulae, the other parameters can be adjusted after the theoretical and experimental powers are in line.

Utilizing experimental data from several PV module technologies, the suggested model is verified. To offer a thorough comparison, the values of current and voltage are computed and graphs are prepared, and the well-known double diode model [15-20]. The global acceptance of photovoltaic solar systems (PV), of which the photovoltaic panel is the primary component, has been greatly aided by government initiatives, and a more than 40% decrease in the price of PV modules was observed in recent years [16-20]. The basic conversion of solar -energy into electrical -energy by a photovoltaic solar panel is contingent upon two factors: temperature of the surrounding environment [20-25] and projected irradiance [23]. Multiple solar cells connected in parallel and series make of up the panels. An accurate (TDM) model based on measured current-voltage (I-V) data is used to assess the accuracy of these solar -cells in the Photovoltaic system [24].

An appropriate mathematical model is required in order to accurately reproduce the electrical behavior of PV solar cells. To mimic this behavior, a variety of models have been put out in the literature; these models usually center on a diode. The single-diode model (SDM) [26], double-diode model (DDM) [27], and more recently, the three-diode model (TDM) for industrial applications [28] are the three primary circuits utilized in the electrical modeling of the PV cell.

1.1 Double-Diode Scheme

Recombination losses are frequently overlooked in the single -diode model of a photovoltaic cell (PV), which results in inaccurate model parameters. As a result, Figure1 illustrates, the double-diode model is used to

more accurately depict the physical properties of the photovoltaic cell (PV). This model takes Recombination loss into Account to increase precision. One of the diodes in the p -n junction material is used to mimic the diffusion -current, and another diode is added to account for recombination loss [28-30].

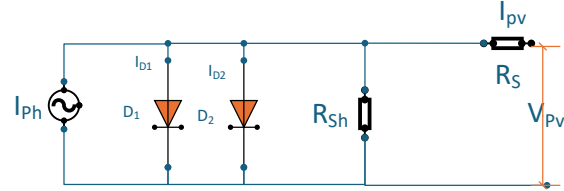


Figure 1 Illustration of conceptual circuit diagram of two-diode model

The PV module's output current can be described as follows:

$$I = I_{ph} - I_o \left[e^{\left(\frac{q(V+IR_s)}{nKNT} \right)} - 1 \right] - I_{sh} \quad (1)$$

Where,

$$I_{ph} = [I_{sc} + (T - 298)] \times \frac{G}{1000} \quad (2)$$

$$I_o = I_{rs} \left[\frac{T}{T_n} \right]^3 e^{\left[\frac{q \cdot E_{go} \left(\frac{1}{T_n} - \frac{1}{T} \right)}{n \cdot K} \right]} \quad (3)$$

$$I_{rs} = \frac{I_{sc}}{e^{\left(\frac{q \cdot V_{oc}}{n \cdot N_s \cdot K \cdot T} \right)} - 1} \quad (4)$$

$$I_{sh} = \left(\frac{V + IR_s}{R_{sh}} \right) \quad (5)$$

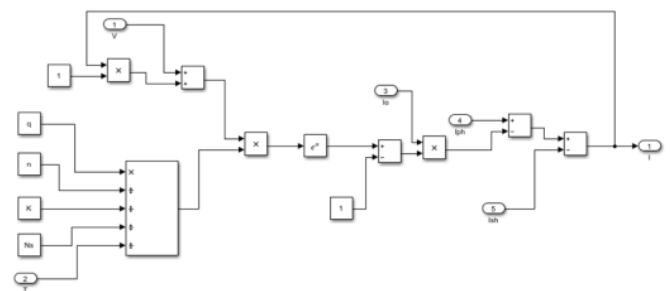


Figure 2 Simulink/Matlab block diagram of output current.

Table 2: The Electrical Basic Parameters of the JAP6- 72 -320/ 4BB Solar P V Module (Source: JAP6 - 72- 320/ 4BB Data Sheet, JA Solar)

S/ N	Parameter (Electrical)	Variable	Value
1	Maximum power at S.T.C (P _m)	P _m	320.00 W
2	Maximum power current (I _{mp})	I _m	08.56 A
3	Maximum power voltage (V _{mp})	V _m	37.38 V
4	Short- circuit current (I _{sc})	I _{sc}	9.06A
5	Open -circuit voltage (V _{oc})	V _{oc}	46.22V
6	Total series cell	N _s	72
7	Ideality factor of the diode	n	1.30
8	Cell short circuit: current temperature coefficient of I _{sc}	K _i	0.058 % °C
9	Basic Reference temperature	T _{ref}	25° C
10	Basic Solar Irradiance	G _{ref}	1000 at S.T.C

2. Methodology

2.1 Analytical method

We can utilize an analytical method based on mathematical analysis and operations based on three basic characteristic points (maximum power points, open-circuit, and short-circuit) at Standard Test Conditions (STC) to extract the parameters of photovoltaic modules. The points and conditions are as follows:

1. Open circuit (OC) point; $I=0$ and $V=V_{oc}$
2. Short circuit (SC) point; $I=I_{sc}$ and $V=0$
3. Maximum power (MP) point; $I=I_m$ and $V=V_m$

2.2 Hybrid Approach to Extracting Parameters

An adjustment is required for more accurate results. The basic goal is to determine the values of R_s , so that, at the maximum power point (V_{mp}, I_{mp}), the main peak that was computed power-voltage ($P-V$) curves that coincide along with these experimental powers peak from the datasheet. Using this procedure, R_s is adjusted iteratively until the theoretical maximum values of power match the datasheet's experimental power value/point.

The experimental and mathematical maximum peak powers should agree at the nominal notable points of the $I-V$ curve, making it possible to calculate the ideal value of V_{max} . Using the analytical equations, the additional parameters will be determined after R_s is

known. The goal is to modify V_{mp} and I_{mp} such that the theoretical maximum power at the maximum power value/ point (V_{mp}, I_{mp}) corresponds to the observed maximum power.

3. The PV Cell Parameters at diverse weather conditions in Naya Raipur Chhattisgarh

The parameters of photovoltaic (PV) modules are subjected to variations in temperature and irradiance due to their operation under a variety of weather scenarios. All parameters, however, are provided under standard test conditions (STC) in Section 3. Extrapolating these parameters for various operating circumstances is crucial.

As stated: (1) The sun illumination at different weather conditions is represented by G (2). The sun illumination at standard (STC) test conditions (1000 W/m^2) is denoted by G_{STC} . (3) The temperature at standard test (STC) conditions (25°C) is denoted by T_{STC} . The observations of solar panels are noted carefully with various environmental facts but we are only using irradiation and temperature values other values like humidity can be controlled by separating solar panel in separate chambers.

4. Result and discussion

4.1 Suggested Framework

The five-parameter analytical method and the seven-parameter hybrid method were the two different methodologies used in this study to systematically evaluate the parameters of photovoltaic (PV) modules. While experimental data was gathered in Naya Raipur, Chhattisgarh, under actual climatic conditions, MATLAB simulations were utilized for parameter extraction and comparison.

The parameters of the Kyocera MSX60 module were obtained using both methods and contrasted with results from previous studies, as indicated in Table 3. Where we lists the features of the Kyocera MSX60 module as well as the other modules used in this study.

Table.2 below consist of the extracted parameters for Kyocera MSX60 for both method containing the result obtained in Naya Raipur for four summer days in the month of July, 2024.

Parameters	Analytical	Hybrid	1 st July	2 nd July	3 rd July	4 th July
I _{ph} (A)	3.810	3.80633	3.8050	3.8081	3.8043	3.8029
I ₀₁ (A)	4.5×10^{-10}	2.5×10^{-11}	3.9×10^{-11}	4.9×10^{-11}	4.2×10^{-11}	4.6×10^{-11}
I ₀₂ (A)	3.01×10^{-9}	3.7×10^{-6}	4.0×10^{-6}	5.9×10^{-1}	4.0×10^{-6}	4.6×10^{-1}
R _s (Ω)	0.35100	0.333	0.331	0.339	0.345	0.368
R _{sh} (Ω)	145.2131	199.60	280.22	170.07	279.567	170.081
n ₁	1	0.9800	0.991	1.002	1	1
n ₂	2	2.0220	2.001	1.998	2	2

4.2 Experimental result.

Through the comparison of experimental data with simulated outcomes, this study work seeks to evaluate the suggested approach for calculating PV panel parameters. An MSX60 PV panel is used to gather data on temperature, voltage, current, and irradiance under various weather conditions over the course of four consecutive sunny days.

Table.3 The values of different parameters for different PV Module

Model	I _{sc} (A)	V _{oc} (V)	I _m (A)	V _m	N _s	K _i (A/K)	K _v (V/K)
MSX60	3.8	21.1	3.5	17.1	36	2.74×10^{-3}	-0.08
ST36	2.68	22.9	2.28	15.8	36	0.32×10^{-3}	-0.100
KC200GT	8.21	32.9	7.61	26.3	54	3.18×10^{-3}	-0.123
ST40	2.68	23.3	2.41	16.6	36	0.35×10^{-3}	-0.100
SM55	3.45	21.7	3.15	17.4	36	1.2×10^{-3}	-0.077
SQ150PC	4.8	43.4	4.4	34	72	1.4×10^{-3}	-0.161

The Kyocera MSX60 PV module was used to gather experimental data over the course of four summer days in July 2024. Temperature, voltage, current, and irradiance were measured at predetermined intervals to examine how the module behaved in different weather scenarios.

Findings from the Experimental Data:

1. As the irradiance grew, the PV power and current rose as well, peaking at noon.

The voltage of the module stayed largely constant, especially in the morning when there were few temperature changes.

The effectiveness of the process is determined by comparing I-V and P-V graphs obtained empirically and through MATLAB Simulink simulations. The experimental components of the PV system are shown in Figure 2, 4 and 5 which show the measurement photos from the experiment. The data collected during the actual deployment is shown in Table 4. The MXS60 PV Module's four-day experimental results for voltage, current, and power are shown. Because there is minimal fluctuation in the ambient air temperature, the PV module's output voltage stays relatively constant during the trial, even with the morning temperature of 20 °C. Mostly as a function of irradiance, the total PV module current peaks at an irradiation of 245 W/m². I-V and P-V characteristics are shown in Figures 4, 5, 6, 7, 8, 9, and 10. In order to illustrate the characteristics of the PV module utilized in this experiment, for each of the four summer days.

Table 4. Four summer days experimental data taken for different temperature and irradiance in Naya Raipur C.G.

Days	Time	Temperature	Irradiance	Current	Voltage	Power
1 st Jul	7:00 am	20	25	0.4	14.1	5.6
	8:00 am	24	73	1.5	13.5	20.25
	9:00 am	27	132	2.9	13.7	39.73
2 nd July	10:00 am	29	180	3.2	13.5	43.20
	11:00 am	30	225	3.5	13.8	48.30
	12:00 pm	31	245	4.0	14.2	56.80
3 rd July	13:00 pm	31	228	4.3	13.9	59.77
	14:00 pm	30	185	3.1	14.2	44.02
	15:00 pm	28	150	2.9	13.6	39.40
4 th July	16:00 pm	24	105	1.4	12.5	17.5
	17:00 pm	22	80	0.4	11.7	4.60
	18:00 pm	20	46	0.1	11.2	1.12

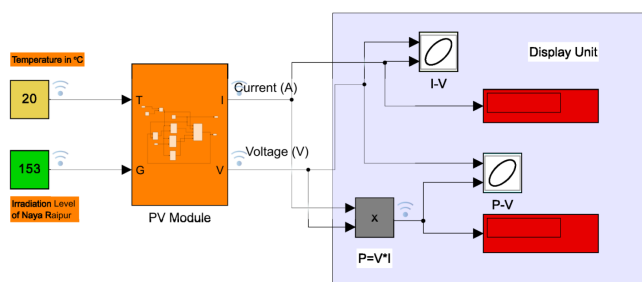


Figure 3 Depicts the complete Simulink model of Final PV Model

The Kyocera MSX60 PV module's I-V and P-V characteristics are displayed in Figure 4 at 27°C and 132 W/m² of irradiance. A typical relationship between current and voltage is shown by the I-V curve, which shows a current of 2.9 A and a voltage of 13.7 V. Current increases as voltage lowers. At this operational point, the P-V curve shows a maximum power output of 39.73 W. This performance validates the simulation model's accuracy in forecasting real-world module behavior and is in line with experimental data gathered on July 1st at 9:00 AM.

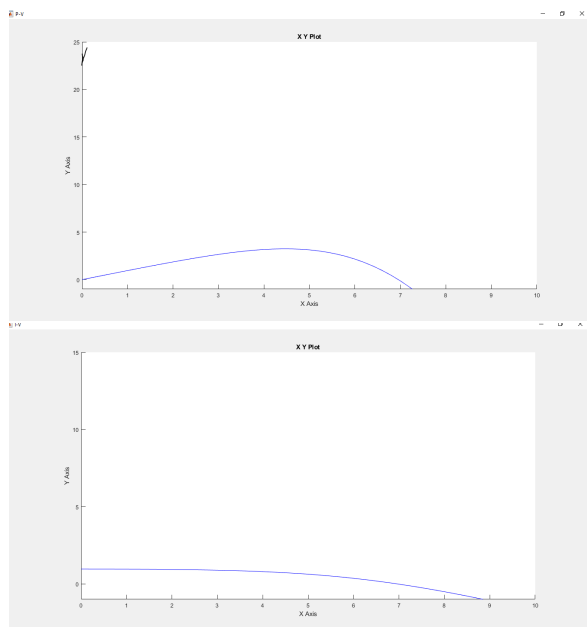


Figure 4 computed I-V and P-V curve at 27 °C temperature and irradiance 132W/m²

Figure 5 illustrates the calculated I-V and P-V characteristics of the Kyocera MSX60 PV module at a

temperature of 31°C and an irradiance of 245 W/m². The I-V curve shows a current of 4.0 A and a voltage of 14.2 V, suggesting an increase in current and voltage compared to lower irradiance levels. As irradiance rises, the current increases while the voltage remains relatively consistent, illustrating the module's excellent conversion of solar energy into electrical power under optimal conditions. The P-V curve demonstrates a peak power production of 56.80 W at this irradiance level, representing a notable enhancement compared to lower irradiance conditions. This performance is commensurate with the experimental data gathered on 2nd July at 12:00 PM, proving the simulation model's accuracy.

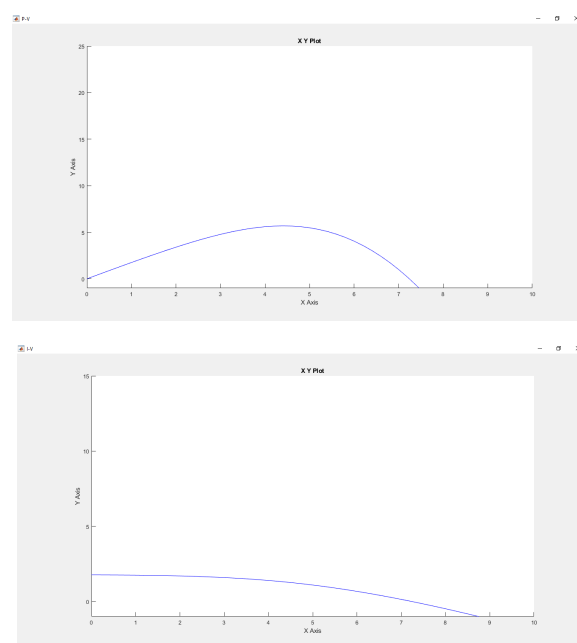


Figure 5 Computed I-V and P-V curve at 31 °C temperature and irradiance 245W/m²

Figure 6 illustrates the computed I-V and P-V characteristics of the Kyocera MSX60 PV module at 30°C temperature and 185 W/m² irradiance. The I-V curve displays a current of 3.1 A and a voltage of 14.2 V. As the irradiance is mild, the current grows with rising irradiance, while the voltage remains relatively consistent. The P-V curve shows a maximum power output of 44.02 W, attained for this combination of temperature and irradiance. The results are congruent with the experimental data acquired on 3rd July at

14:00 PM, verifying the accuracy of the simulation. This research illustrates the module's good performance under moderate temperature and irradiance circumstances, demonstrating a solid power output when subjected to average midday sunlight.

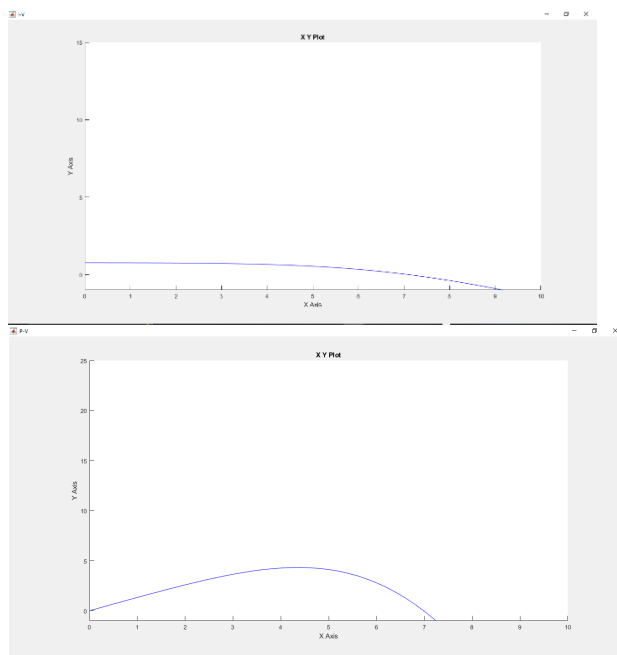


Figure 6 Computed I-V and P-V curve at 30 °C and irradiance 185W/m²

Figure 7 illustrates the computed I-V and P-V characteristics of the Kyocera MSX60 PV module at 24°C temperature and 105 W/m² irradiance. The I-V curve indicates a current of 1.4 and a voltage of 12.5 V, with a considerable drop in current and voltage compared to higher irradiation circumstances. As expected, under decreased irradiance, the module provides a lesser current, and the voltage marginally falls as well. The P-V curve suggests a maximum power output of 17.50 W at this irradiation level. These findings are congruent with the experimental data acquired on 4th July at 16:00 PM, demonstrating the accuracy of the simulation.

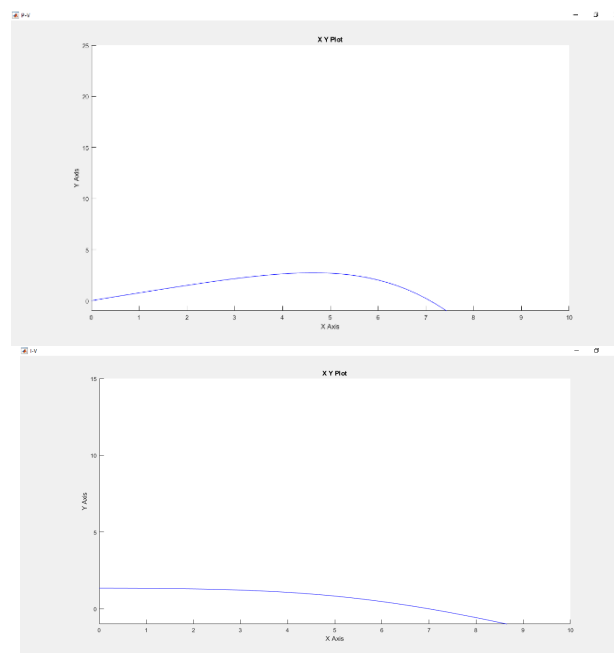


Figure 7 Computed I-V and P-V curve at 24 °C temperature and irradiance 105W/m²

The experimental voltage of the Kyocera MSX60 PV panel is recorded under varying conditions of temperature and irradiance. The data for voltage collected during the experiment on the 1st to 4th of July shows that the voltage remains relatively steady, with slight variations depending on the irradiance and temperature levels. For example, at **7:00 AM on 1st July**, the temperature is 20°C and irradiance is 25 W/m², the voltage is measured at **14.1 V**, while at **12:00 PM on 2nd July**, under 245 W/m² irradiance and 31°C, the voltage is **14.2 V**. Despite fluctuations in irradiance and temperature, the voltage generally stays within a narrow range (approximately 13.5 V to 14.2 V), reflecting the stable operating nature of the PV panel under these conditions. The voltage does not exhibit significant changes, indicating that the module's voltage output is more stable than its current under varying environmental conditions.

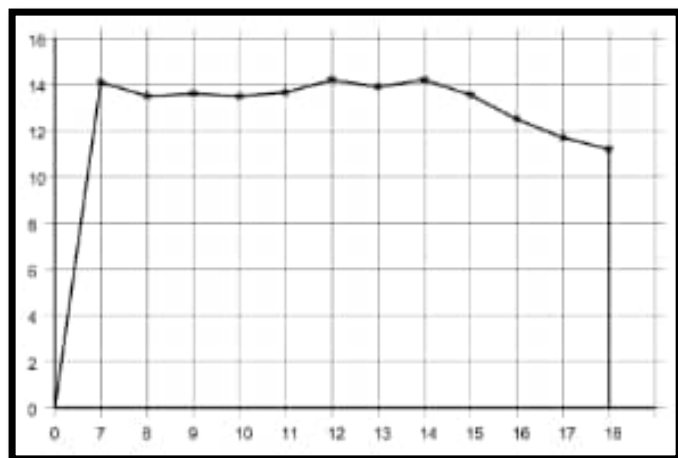


Figure 8 Experimental voltage of the PV panel

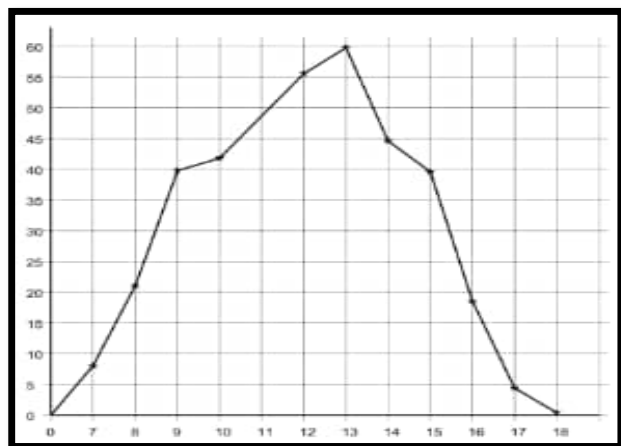


Figure 9 Experimental current of the PV Panel

Figure 9 illustrates the experimental current data of the Kyocera MSX60 PV panel under changing temperature and irradiation circumstances. The current displays a clear dependency on irradiance levels, with higher irradiance correlating to increased current output. For instance, at 7:00 AM on 1st July, when the temperature is 20°C and irradiance is 25 W/m², the current is measured at 0.4 A, whereas at 12:00 PM on 2nd July, under higher irradiance of 245 W/m² and a temperature of 31°C, the current jumps to 4.0 A. This rise in current with growing irradiance is consistent with the expected behavior of photovoltaic modules, which generate greater current when exposed to higher levels of sunshine. Throughout the experiment, the current fluctuates as a result of various weather conditions,

but the general trend clearly demonstrates that the current is strongly connected with both irradiance and temperature, indicating the module's response to changes in environmental parameters.

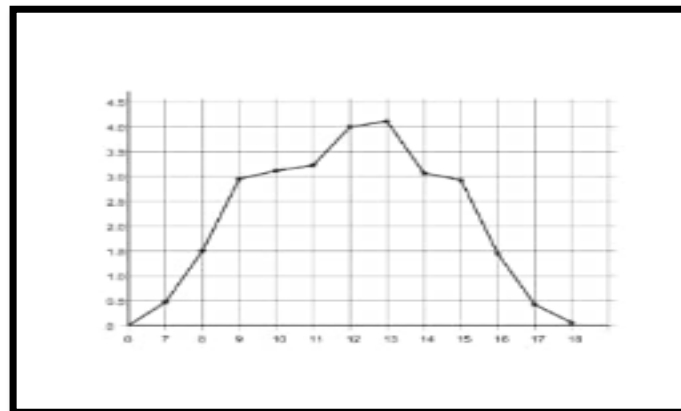


Figure 10 Experimental power of the PV Panel.

Figure 10 displays the experimental power output of the Kyocera MSX60 PV panel under changing temperature and irradiation conditions. The power production is directly impacted by the current and voltage, both of which depend on the irradiance and temperature. For instance, at 7:00 AM on 1st July, with a temperature of 20°C and irradiance of 25 W/m², the power output is 5.64 W. As the irradiance increases, particularly on 2nd July at 12:00 PM under 245 W/m² irradiance and 31°C temperature, the power output reaches a peak of 56.80 W. The power output continually improves with greater irradiance, illustrating the module's efficient conversion of solar energy to electricity. On the other hand, when irradiance declines, such as at 16:00 PM on 4th July with 105 W/m², the power output is significantly lower at 17.50 W. Overall, the power production follows a predictable trend of increasing with higher irradiance and temperature, with the module achieving ideal performance under peak sunshine circumstances. This steady association supports the reliability of the PV module under diverse real-world settings.

5. Conclusion

This paper provided a hybrid methodology for extracting features of the two-diode model (TDM) for photovoltaic (PV) modules that was suited to the environmental circumstances of Naya Raipur, Chhattisgarh. Key features, such as series resistance ($R_s = 0.333\text{--}0.368\ \Omega$), shunt resistance ($R_h = 170.07\text{--}280.22\ \Omega$), and ideality factors ($n_1 = 0.980\text{--}1.002$, $n_2 = 2.001\text{--}2.022$), were precisely calculated by the use of numerical optimization and analytical models. A maximum power production of 59.77 W was reported in experimental data obtained over four summer days (temperature: $20^\circ\text{C}\text{--}31^\circ\text{C}$, irradiance: $25\text{--}245\ \text{W/m}^2$). Root mean square error (RMSE) values for this experimental data were less than 1%, which was in close according to MATLAB/Simulink simulations. $I_{sr} = 9.06\ \text{A}$, $V_o^c = 46.22\ \text{V}$, $V_{mp} = 37.38\ \text{V}$, and $I_{mp} = 8.56\ \text{A}$, were among the parameters of the Kyocera MSX60 module. The temperature coefficients for voltage ($K_v = -0.077\ \text{to}\ -0.161\ \text{V/K}$) and current ($K_i = 1.2 \times 10^{-3}\ \text{to}\ 3.18 \times 10^{-3}\ \text{A/K}$) exhibited high adaptation to local conditions. According to the results, this trustworthy and expandable hybrid strategy bridges the gap between theoretical modeling and real performance by offering precise performance forecasts for PV systems in a range of climatic scenarios.

References.

- [1] "Characteristics and Connections of Cells, Modules, and Arrays," 2012.
- [2] Bagher, A.M., Vahid, M.M.A., & Mohsen, M., "Types of Solar Cells and Their Applications," *American Journal of Optics and Photonics*, vol. 3, no. 5, pp. 94–113, 2015.
- [3] Barth, N., Jovanovic, R., Ahzi, S., & Khaleel, M.A., "PV Panel Single and Double Diode Models: Optimization of the Parameters and Temperature Dependence," *Solar Energy Materials & Solar Cells*, vol. 148, pp. 87–98, 2016.
- [4] Bellia, H., "A Detailed Modeling of Photovoltaic Module Using MATLAB," *NRIAG Journal of Astronomy and Geophysics*, vol. 3, no. 1, pp. 53–61, 2014.
- [5] Brihmat, F., & Mekhtoub, S., "PV Cell Temperature/PV Power Output Relationships Homer Methodology Calculation," *International Journal of Scientific Research and Engineering Technology*, vol. 2, no. 1, 2014.
- [6] Elbaset, A.A., Ali, H., & Abd-El Sattar, M., "Novel Photovoltaic Module Model with Seven Parameters," *Solar Energy Materials & Solar Cells*, vol. 130, pp. 442–455, 2014.
- [7] Farzaneh, J., Keypour, R., & Khanesar, M.A., "A New Maximum Power Point Tracking Based on Modified Firefly Algorithm for PV System Under Partial Shading Conditions," *Technology Economics of Smart Grids and Sustainable Energy*, vol. 3, no. 1, pp. 1–13, 2018.
- [8] Guo, T., Yang, G., Wang, S., & Lun, S., "A Fresh, Clear Double Modeling Technique for Solar Panels Based on the Lambert W-function," *Solar Energy*, vol. 116, pp. 69–82, 2015.
- [9] Hejri, M., Mokhtari, M.R., Azizian, M.R., & Soder, L., "Extraction of Parameters from a Five-Parameter Double-Diode Model of Solar Cells and Modifications," *Solar Energy Materials & Solar Cells*, vol. 130, pp. 442–455, 2014.
- [10] Hersch, P., & Zweibel, K., "Basic Photovoltaic Principles and Methods," *Antimicrobial Agents and Chemotherapy*, vol. 58, no. 12, pp. 7250–7257, 1982.
- [11] Hovinen, A., "Fitting of the Solar Cell I-V Curve to the Two-Diode Model," *Physics Scripta*, T. 54, 2, 1994.
- [12] Imamzai, M., Aghaei, M., Thayoob, Y.H.M., & Forouzanfar, M., "A Review on Comparison Between Traditional Silicon Solar Cells and Thin-Film CdTe Solar Cells," *National Graduate Conference Proceedings*, pp. 1–5, 2012.
- [13] International Agency for Renewable Energy, "Solar Photovoltaic Future," November 2019. [PDF document].
- [14] International Renewable Energy Agency, "Renewable Capacity Highlights," March 2020. [PDF document].
- [15] Ishaque, K., Salam, Z., & Taheri, H., "Accurate MATLAB Simulink PV System Simulator Based on a Two-Diode Model," *Journal of Power Electronics*, vol. 11, no. 2, pp. 179–187, 2011.
- [16] Jumaat, S.A., & Crocker, F., "Investigate the Photovoltaic (PV) Module Performance Using Artificial Neural Network (ANN)," *IEEE Conference on Open Systems (ICOS)*, Langkawi, 2016.
- [17] Kermadi, M., & Berkouk, E.M., "Artificial Intelligence-Based Maximum Power Point Tracking Controllers for Photovoltaic Systems: A Comparative Study," *Renewable & Sustainable Energy Reviews*, vol. 69, pp. 369–386, 2017.
- [18] Kumar, M., & Kumar, A., "A Proficient Method for Extracting Characteristics from Photovoltaic Models for Evaluating Performance," *Solar Energy*, vol. 158, pp. 192–206, 2017.
- [19] Laudani, A., Riganti Fulginei, F., & Salvini, A., "Identification of the One-Diode Model for Photovoltaic Modules from Datasheet Values," *Solar Energy*, vol. 108, pp. 432–446, 2014.
- [20] McDonald, K., "Solar Electricity for Over One Billion People and Two Million Jobs by 2020," *Greenpeace International*, Report No. 1, 2006.
- [21] Mohammed, S.S., "Modeling and Simulation of Photovoltaic Module Using MATLAB/Simulink," *International Journal of Chemical and Environmental Engineering*, vol. 2, no. 5, 2011.

- [22] Motahhir, S., Chalh, A., Ghzizal, A., Sebti, S., & Derouich, A., "Modeling of Photovoltaic Panel by Using Proteus," *Journal of Engineering Science & Technology*, vol. 5, no. 3, 2015.
- [23] Pellet, N., et al., "Hill Climbing Hysteresis of Perovskite-Based Solar Cells: A Maximum Power Point Tracking Investigation," *Progress in Photovoltaics: Research and Applications*, vol. 25, no. 11, pp. 942–950, 2017.
- [24] Phang, J.C., & Chan, D.S., "Techniques for Analytically Deriving Single- and Double-Diode Model Parameters for Solar Cells from IV Features," *IEEE Transactions on Electronic Devices*, vol. 34, no. 2, pp. 286–293, 1987.
- [25] Salam, Z., Ishaque, K., & Chin, V. J., "An Accurate Differential Evolution-Based Hybrid Solution for the Two-Diode Model of a Photovoltaic Panel," *Energy Conversion and Management*, vol. 124, pp. 42–50, 2016.
- [26] Salam, Z., Ishaque, K., & Taheri, H., "The Two-Diode Model for Photovoltaic Modules: A Straightforward, Quick, and Precise Approach," *Solar Energy Materials & Solar Cells*, vol. 95, no. 2, pp. 586–594, 2011.
- [27] Saleh, A.L., Obed, A.A., Hassoun, Z.A., & Yaqoob, S.J., "Modeling and Simulation of Low-Cost Perturb & Observe and Incremental Conductance MPPT Techniques in Proteus Software Based on Flyback Converter," *IOP Conference Series: Materials Science and Engineering*, vol. 881, no. 1, p. 012152, 2020.
- [28] Tsai, H., et al., "Development of Generalized Photovoltaic Model Using MATLAB/Simulink," *World Congress on Engineering and Computer Science (WCECS)*, San Francisco, 2008.
- [29] Vachtsevanos, G., & Kalaitzakis, K., "A Hybrid Photovoltaic Simulator for Utility Interactive Studies," *IEEE Transactions on Energy Conversion*, vol. 2, pp. 227–231, 1987.
- [30] Vedanayakam, S.V., et al., "A Detailed MATLAB Modeling of Photovoltaic Module," *International Journal of Industrial Electronics and Electrical Engineering*, vol. 4, no. 10, pp. 28–32, 2016.
- [31] Villalva, M. G., Gazoli, J. R., & Filho, E. R., "Comprehensive Approach to Modeling and Simulation of Photovoltaic Arrays," *IEEE Transactions on Power Electronics*, vol. 94, no. 5, 2009.
- [32] Walker, G., "Evaluating MPPT Converter Topologies Using a MATLAB PV Model," *Journal of Electrical & Electronic Engineering*, vol. 21, pp. 49–56, 2001.
- [33] Zainal, N.A., "Modeling of Photovoltaic Module Using MATLAB Simulink," *IOP Conference on Materials Science and Engineering*, Pahang, 2016.